

Published in final edited form as:

Cell Physiol Biochem. 2019 ; 52(1): 57–75. doi:10.33594/000000005.

Glycogen Synthase Kinase 3 Beta Controls Presenilin-1-Mediated Endoplasmic Reticulum Ca²⁺ Leak Directed to Mitochondria in Pancreatic Islets and β -Cells

Christiane Klec^a, Corina T. Madreiter-Sokolowski^a, Sarah Stryeck^a, Vinay Sachdev^{a,b}, Madalina Duta-Mare^a, Benjamin Gottschalk^a, Maria R. Depaoli^a, Rene Rost^a, Jesse Hay^{a,c}, Markus Waldeck-Weiermair^a, Dagmar Kratky^{a,d}, Tobias Madl^{a,d}, Roland Malli^{a,d}, and Wolfgang F. Graier^{a,d}

^aMolecular Biology and Biochemistry, Gottfried Schatz Research Center for Cellular Signaling, Metabolism & Aging, Medical University of Graz, Graz, Austria ^bDepartment of Medical Biochemistry, Academic Medical Center, University of Amsterdam, Amsterdam, The Netherlands ^cUniversity of Montana, Division of Biological Sciences, Center for Structural & Functional Neuroscience, Missoula, MT, USA ^dBioTechMed, Graz, Austria

Abstract

Background/Aims—In pancreatic β -cells, the intracellular Ca²⁺ homeostasis is an essential regulator of the cells' major functions. The endoplasmic reticulum (ER) as interactive intracellular Ca²⁺ store balances cellular Ca²⁺. In this study basal ER Ca²⁺ homeostasis was evaluated in order to reveal potential β -cell-specificity of ER Ca²⁺ handling and its consequences for mitochondrial Ca²⁺, ATP and respiration.

Methods—The two pancreatic cell lines INS-1 and MIN-6, freshly isolated pancreatic islets, and the two non-pancreatic cell lines HeLA and EA.hy926 were used. Cytosolic, ER and mitochondrial Ca²⁺ and ATP measurements were performed using single cell fluorescence microscopy and respective (genetically-encoded) sensors/dyes. Mitochondrial respiration was monitored by respirometry. GSK3 β activity was measured with ELISA.

Results—An atypical ER Ca²⁺ leak was observed exclusively in pancreatic islets and β -cells. This continuous ER Ca²⁺ efflux is directed to mitochondria and increases basal respiration and organellar ATP levels, is established by GSK3 β -mediated phosphorylation of presenilin-1, and is prevented by either knockdown of presenilin-1 or an inhibition/knockdown of GSK3 β . Expression of a presenilin-1 mutant that mimics GSK3 β -mediated phosphorylation established a β -cell-like

This article is licensed under the Creative Commons Attribution-NonCommercial-NoDerivatives 4.0 International License (CC BY-NC-ND). Usage and distribution for commercial purposes as well as any distribution of modified material requires written permission (<http://creativecommons.org/licenses/by/4.0/>).

Wolfgang F. Graier, Molecular Biology and Biochemistry, Gottfried Schatz Research Center for Cellular Signaling, Metabolism & Aging, Medical University of Graz, Neue Stiftingtalstraße 6/VI, 8010 Graz (Austria) Tel. +43 316 385 71963, wolfgang.graier@medunigraz.at.

Disclosure Statement

The authors declare no competing financial interests.

ER Ca²⁺ leak in HeLa and EA.hy926 cells. The ER Ca²⁺ loss in β -cells was compensated at steady state by Ca²⁺ entry that is linked to the activity of TRPC3.

Conclusion—Pancreatic β -cells establish a cell-specific ER Ca²⁺ leak that is under the control of GSK3 β and directed to mitochondria, thus, reflecting a cell-specific intracellular Ca²⁺ handling for basal mitochondrial activity.

Keywords

Mitochondria; Ca²⁺ leak; Endoplasmic reticulum Ca²⁺; Insulin release; Respiration; Presenilin-1

Introduction

The occurrence of type 2 diabetes mellitus (DM), characterized by insulin resistance and pancreatic β -cell dysfunction, is rapidly increasing worldwide and is associated with increased morbidity and mortality [1, 2]. The predominant function of pancreatic β -cells is the control of blood glucose levels by the regulated secretion of sufficient amounts of insulin. Insulin production and release are tightly controlled by mainly glucose, several peptide hormones, neurotransmitters and other nutrients under physiological conditions [3]. On the molecular level, elevations in blood glucose are sensed in pancreatic β -cells via efficient uptake and subsequent catabolism of glucose, leading to an increase in mitochondrial ATP production. Subsequently, elevated intracellular ATP levels inhibit K_{ATP} channels, leading to plasma membrane depolarization and Ca²⁺ influx via L-type Ca²⁺ channels. This stimulated Ca²⁺ entry directly results in exocytosis of insulin-containing secretory granules [4]. Recently, it was shown that mitochondrial Ca²⁺ uptake is also crucial for activation of glucose stimulated insulin secretion (GSIS) [5, 6]. Indeed, it was demonstrated that mitochondrial Ca²⁺ sequestration in clonal pancreatic β -cells supports GSIS [7, 8]. In line with this assumption, two mitochondrial proteins, namely the mitochondrial Ca²⁺ uniporter (MCU) [9, 10] and the mitochondrial Ca²⁺ uptake 1 (MICU1), known for their role in mitochondrial Ca²⁺ uptake [11], were shown to be essential for pancreatic β -cell function [12]. However, the current concepts explain only how elevated mitochondrial Ca²⁺ uptake could promote insulin secretion once Ca²⁺ entry is already activated by elevated ATP levels, and do not address its required role in the production of the elevated ATP at the triggering stage. It is, entirely unclear whether or not, and if so, how the resting mitochondrial Ca²⁺ homeostasis of pancreatic β -cells contributes to the initial glucose sensing process. Recently, it was speculated that a pre-activation of mitochondria in pancreatic β -cells during fasting is required for efficient glucose sensing once blood glucose levels increase [13]. In this context it was speculated that low levels of continuous glucose uptake and metabolism, other nutrients, hormones and/or neural stimulation weakly pre-activate pancreatic β -cell mitochondria during fasting. While this concept appears convincing as such and pre-stimulation of mitochondria would allow the organelle to immediately respond to increased rates of glycolysis, the underlying molecular mechanisms remain elusive.

In the present study we sought to explore *i*, the potential β -cell specific characteristics in the resting Ca²⁺ handling of the ER, *ii*, its impact on basal mitochondrial Ca²⁺, and, *iii*, their consequences on mitochondrial respiration. We used the two widely-used β -cell lines INS-1

[14] and MIN-6 [15], and freshly isolated mouse pancreatic islets and compared the Ca^{2+} tightness/leakage kinetics of their ER and basal mitochondrial Ca^{2+} homeostasis with that of the two non- β -cell lines, HeLa [16] and EA.hy926 [17]. Cytosolic, mitochondrial and ER Ca^{2+} measurements using either Fura-2 or organelle-targeted genetically encoded Ca^{2+} sensors on single cell fluorescence imaging microscopes were applied [12, 18]. The impact on mitochondrial respiration was examined using Seahorse[®] technology [19] and ELISA was used to verify phosphorylation and enzymatic activity. Applying such technological variety, we were able to identify β -cell specificities in resting ER Ca^{2+} handling that, subsequently, impacts mitochondrial basal Ca^{2+} levels and the organelle's respiratory activity.

Materials and Methods

Reagents

Cell culture materials were obtained from Greiner Bio-One (Kremsmünster, Austria). Histamine (His; PubChem CID: 774), antimycin A (PubChem CID: 16218979), oligomycin A (PubChem CID: 5281899), carbonyl cyanide p-trifluoromethoxyphenylhydrazone (FCCP; PubChem CID: 3330), 2, 5-di-*t*-butyl-1, 4-benzohydroquinone (BHQ; PubChem CID: 16043), ethylene glycol tetraacetic acid (EGTA; PubChem CID: 6207), carbachol (Cch; PubChem CID: 5832), efonidipine hydrochloride monoethanolate (PubChem CID: 163838), *N*-[4-[3, 5-Bis(trifluoromethyl)-1*H*-pyrazol-1-yl]phenyl]-3-fluoro-4-pyridinecarboxamide (Pyr6; PubChem CID: 10596093) and *N*-(4-(3, 5-bis(trifluoromethyl)-1*H*-pyrazole-1-yl)phenyl)-4-methylbenzenesulfonamide (Pyr10; PubChem CID: 53475435) were purchased from Sigma Aldrich (Vienna, Austria). The selective GSK3 β inhibitor 6-[[2-[[4-(2, 4-Dichlorophenyl)-5-(5-methyl-1*H*-imidazol-2-yl)-2-pyrimidinyl]amino]ethyl]amino]-3-pyridinecarbonitrile (CHIR99021; PubChem CID: 9956119) was purchased from Tocris (Bristol, UK). Acetyloxymethyl 2-[6-[bis [2-(acetyloxymethoxy)-2-oxoethyl] amino]-5-[2-[2-[bis [2-(acetyloxymethoxy)-2-oxoethyl]amino]-5-methylphenoxy]ethoxy]-1-benzofuran-2-yl]-1, 3-oxazole-5-carboxylate (Fura-2/AM; PubChem CID: 3364574) was from MoBiTec GmbH (Göttingen, Germany) or TEFLabs (Austin, TX, USA). Unless otherwise specified, genetically-encoded fluorescence sensors were purchased either from Addgene (Cambridge, MA 02139, USA) or Next Generation Fluorescence Imaging, NGFI, Graz, Austria (www.ngfi.eu). Other chemicals were from Carl Roth (Karlsruhe, Germany).

Isolation of murine pancreatic islets

For all experiments, age-matched male C57BL/6 mice purchased from Jackson Laboratory (Bar Harbor, ME) between 3-4 months of age were used. Mice were fed regular chow diet (11.9% caloric intake from fat; Altromin 1324, Lage, Germany) and maintained in a 12:12-h light-dark cycle in a temperature-controlled environment. All animal experiments were carried out in accordance with the guidelines set by the Division of Genetic Engineering and Animal Experiments and were approved by the Austrian Federal Ministry of Science, Research, and Economy (Vienna, Austria). Murine islets were isolated as described [20].

Cell culture and transfection

INS-1 832/13 (INS-1) cells were a generous gift from Prof. Dr. Claes B. Wollheim and Dr. Françoise Assimacopoulos-Jeannet (University Medical Center, Geneva, Switzerland). INS-1 cells were cultured in RPMI 1640 containing 11 mM glucose (PubChem CID: 5793) supplemented with 10 mM HEPES (PubChem CID: 23831), 10% fetal calf serum (FCS), 1 mM sodium pyruvate (PubChem CID: 23662274), 50 μ M β -mercaptoethanol (PubChem CID: 1567), 1% (v/v) Pen Strep® (ThermoFischer, Vienna, Austria; 10.000 U/L). MIN-6 cells (ATCC® CRL-11506™) were cultured in DMEM supplemented with 25 mM glucose, 10 mM HEPES, 10% FCS, 1 mM sodium pyruvate, 50 μ M β -mercaptoethanol, 50 μ g penicillin and 100 μ g streptomycin. HeLa and EA.hy926 cells were grown in Dulbecco's Modified Eagle Medium (DMEM) supplemented with 10% fetal bovine serum (FBS), 100 U/ml penicillin and 100 μ g/ml streptomycin as well as 2 mM glutamine (PubChem CID: 5961) (Gibco, Life Technologies, Vienna Austria), designated as full DMEM. Origin of cells was confirmed by STR-profiling by the cell culture facility of ZMF (Graz).

Transfection with siRNAs and plasmids

For Ca^{2+} imaging, cells were plated on 30 mm glass coverslips in 6-well plates and transiently transfected at 60 - 80% confluency with 1.5 μ g plasmid DNA alone or with 100 nM siRNA using 2.5 μ l TransFast transfection reagent (Promega, Madison, WI, USA) in 1 ml of serum- and antibiotic-free medium. Cells were maintained in a humidified incubator (37°C, 5% CO_2 , 95% air) for 16-20 h. Thereafter, the transfection mix was replaced by full culture medium. For treatment with the GSK3 β inhibitor CHIR99021 cells were incubated in their respective media containing 2.5 μ M CHIR99021. All experiments were performed 24 - 48 h after transfection or treatment. siRNAs were obtained from Microsynth (Balgach, Switzerland) or ThermoFisher Scientific (Vienna, Austria). Sequences are listed in Supplementary Table 1 (all supplementary material available online at www.cellphysiolbiochem.com). Presenilin-1 wild type as well as the mutant versions presenilin-1^{S353/357A} and presenilin-1^{S353/357D} overexpression plasmids were designed by us and synthesized by General Biosystems (Morrisville, USA). All presenilin-1 versions were cloned into a pcDNA3.1 backbone and are flanked by XbaI and EcoRI restriction sites. Cells were transfected with an excessive amount of siRNA vs. the respective fluorescent sensor (ratio of 2.5×10^9 mol siRNA: 1 mol plasmid) to ensure the transfection of the siRNA in cells positively transfected with the fluorescent sensor as the cells used for single cell recordings.

mRNA Isolation, real time and detection PCRs

Total RNA isolation, reverse transcription, PCR and real-time-PCR were performed according our recently published protocols [18]. Relative expression of specific genes was normalized to human, rat or mouse GAPDH, as a housekeeping gene. Primers for real-time PCR and detection PCR were obtained from Invitrogen (Vienna, Austria). The respective primer sequences are listed in Supplementary Table 1 (For all supplemental material see www.karger.com/doi/).

Total and pS9 GSK3 β enzyme-linked immunosorbent assay (ELISA)

To determine the levels of total and pS9 (inactive) GSK3 β the ELISA kit ab205711 (Abcam, Cambridge, UK) was used. In short, MIN-6, INS-1, HeLa and EA.hy926 cells were cultured until they reached approx. 80% confluency and lysed with the lysis buffer supplied with the kit. Protein concentration was measured using the PierceTM BCA Protein Assay Kit (ThermoFisher Scientific) and 5 μ g protein were used for the ELISA. The remaining procedure was performed according to the manufacturer's protocol.

Mitochondrial respiration measurements

INS-1, MIN-6, HeLa and EA.hy926 cells, treated or not with siRNA against presenilin-1 or GSK3 β inhibitor CHIR99021, were plated in XF96 polystyrene cell culture microplates (Seahorse Bioscience) at a density of 60.000 cells/well for HeLa and EA.hy926, 120.000 cells/well for MIN-6 and 140.000 cells/well for INS-1 cells. After overnight incubation, mitochondrial respiration was performed using an XF96 extracellular flux analyzer (Seahorse Bioscience[®]) as previously described [21]. Oxygen consumption was normalized to protein content (pmol O₂/min \times μ g protein).

Calcium imaging of isolated murine pancreatic islets

Islets were treated with 2.5 μ M CHIR99021 or DMSO as control as described above. The next day islets were washed once with experimental buffer (EB; containing 135 mM NaCl, 5 mM KCl, 2 mM CaCl₂, 1 mM MgCl₂, 10 mM Hepes, 2.6 mM NaHCO₃, 440 μ M KH₂PO₄, 340 μ M Na₂HPO₄, 10 mM glucose, 0.1% vitamins, 0.2% essential amino acids, and 1% penicillin-streptomycin (all v/v); pH adjusted to 7.4) and loaded with 2 μ M Fura-2/AM in EB for 40 min as previously described [12]. After washing once with EB buffer, islets were transferred on a 35 mm ibidi single imaging dish with glass bottom (ibidi, Munich, Germany) in 1.5 ml of 0 Ca buffer (i.e. EB buffer without CaCl₂ added plus 1 mM EGTA) and immediately imaged or kept on 0 Ca buffer for 20 min and imaged afterwards. To initiate ER Ca²⁺ release islets were stimulated by adding 500 μ l 0 Ca buffer containing carbachol and BHQ to reach final concentrations of 100 μ M and 15 μ M, respectively.

Cytosolic Ca²⁺ imaging in cultured β -cells

Cells were loaded with 2 μ M Fura-2/AM (TEFLabs) in EB for 40 min and were alternately illuminated at 340 and 380 nm, whereas fluorescence emission was recorded at 510 nm {Alam:2012bo}[12] {Alam:2012bo}. Results of Fura-2/AM measurements are shown as the ratio of F₃₄₀/F₃₈₀. For titration of cytosolic Ca²⁺ to visualize ER Ca²⁺ leak, after Fura-2/AM loading, cells were incubated for the indicated times in an experimental buffer without Ca²⁺ consisting of 138 mM NaCl, 1 mM MgCl₂, 5 mM KCl, 10 mM Hepes, 10 mM glucose and 1 mM EGTA and subsequently stimulated with 100 μ M of IP₃-generating agonists (INS-1 and MIN-6: carbachol, HeLa and EA.hy926: histamine) in the presence of 15 μ M of the SERCA inhibitor BHQ. For glucose-induced cytosolic Ca²⁺ measurements, cells were loaded with 2 μ M Fura-2/AM as described previously [12]. Briefly, prior imaging cells were incubated for 20 min incubation in glucose free buffer (0G; 10 mM mannitol to osmotically substitute the glucose). On the microscope, cells were perfused with 0G buffer for 2 min before switching to 16 mM glucose (16G) during acquisition. To evaluate the

maximal Ca^{2+} uptake via L-type Ca^{2+} channels, cells were depolarized with a high K^+ buffer, where 25 mM NaCl were substituted with KCl.

FRET measurements using genetically encoded sensors

$[\text{Ca}^{2+}]_{\text{mito}}$, $[\text{Ca}^{2+}]_{\text{ER}}$ and $[\text{ATP}]_{\text{mito}}$ were measured in cells expressing 4mtD3cpv, D1ER and mtAT1.03, as previously described [12, 22].

Statistical analyses

Data shown represent the mean \pm SEM. 'n' values refer to the number of individual experiments performed. For live cell imaging numbers indicate the numbers of cells/independent repeat. If applicable, analysis of variance (ANOVA) was used for data evaluation and statistical significance of differences between means was estimated by Bonferroni *post hoc* test or two-tailed Student's t-test using GraphPad Prism 5.0f (GraphPad Software, La Jolla, CA, USA).

Results

Pancreatic islets and β -cells display an atypical ER Ca^{2+} leakage

To seek for potential β -cell specific characteristics in the resting Ca^{2+} handling of the ER, we compared the potential ER Ca^{2+} leakage in freshly isolated murine pancreatic islets and the two β -cell lines, INS-1 [14] and MIN-6 [15], with that of the two distinct widely studied non- β -cell lines, HeLa [16] and EA.hy926 [17]. To this end, extracellular Ca^{2+} was removed from cells and the ER Ca^{2+} content was indirectly estimated from cytosolic Ca^{2+} elevations upon ER Ca^{2+} -mobilization with an inositol-1, 4,5-trisphosphate- (IP_3 -) generating agonist (either by 100 μM carbachol [Cch] in pancreatic islets and β -cells or 100 μM histamine [His] in the non- β -cells) in presence of the reversible SERCA inhibitor tert-butylhydroxyquinone (BHQ, to avoid ER Ca^{2+} refilling) (Fig. 1A). By applying this protocol we detected a massive ER Ca^{2+} loss after 20 min in Ca^{2+} -free buffer in isolated pancreatic islets (Fig. 1B) and both β -cell lines (Fig. 2A), whereas there was no detectable net ER Ca^{2+} loss during 20 min in a Ca^{2+} -free environment in HeLa and EA.hy926 cells (Fig. 2B). Determination of the ER Ca^{2+} content utilizing the ER-targeted genetically encoded sensor, D1ER [23], confirmed the existence of a β -cell-specific enhanced ER Ca^{2+} loss upon removal of extracellular Ca^{2+} (Fig. 3A).

In contrast to the robust ER Ca^{2+} maintenance seen in HeLa and EA.hy926, maintenance of ER Ca^{2+} in β -cells was entirely dependent upon extracellular Ca^{2+} (Fig. 3B). Furthermore, upon removal of BHQ and Cch, and re-addition of extracellular Ca^{2+} , ER Ca^{2+} levels were rapidly restored in pancreatic β -cells. These results reveal a pancreatic islets/ β -cell-specific strong ER Ca^{2+} leakage that is normally compensated by continuous ER Ca^{2+} replenishment, which is in turn fueled by extracellular Ca^{2+} entry (Fig. 3B).

β -cells specific ER Ca^{2+} leakage is compensated by continuous TRPC3-associated Ca^{2+} entry

To determine the mechanisms involved in the compensation of enhanced ER Ca^{2+} depletion in clonal pancreatic β -cells by extracellular Ca^{2+} , the potential contribution of store-operated

Ca²⁺ entry (SOCE) via Orai1, the transient receptor potential channel 3 (TRPC3) and the L-type Ca²⁺ channels (L-TCC) was examined. Initially, we approached this issue by using pharmacological inhibitors. Specifically, we determined the ER Ca²⁺ content of pancreatic β -cells in Ca²⁺-containing buffer in the presence of 20 μ M efonidipine [24], 1 or 40 μ M Pyr6, and 3 μ M Pyr10 [25] to inhibit Ca²⁺ entry via L-TCC, Orai1 and TRPC3, respectively. In contrast to efonidipine and 1 μ M Pyr6 treatment, that did not affect the ER Ca²⁺ content of the β -cells (Suppl. Fig. 1), the inhibition of TRPC3 by 40 μ M Pyr6 or 3 μ M Pyr10 yielded a consistent ER Ca²⁺ depletion (Fig. 4A). To support these findings, TRPC3 expression was specifically reduced with siRNA and the ER Ca²⁺ content was evaluated. Treatment with siRNA yielded significantly reduced TRPC3 expression levels by 12 and 18 h post transfection with siRNA (Suppl. Fig. 2). The diminution of TRPC3 expression was associated with a reduction of ER Ca²⁺ content 12 and 18 h after transfection (Fig. 4B). Longer transfection periods negatively impacted cell survival, probably due to the continuous ER Ca²⁺ depletion and initiation of ER stress-induced cell death. These results suggest that in the presence of extracellular Ca²⁺, ER Ca²⁺ leakage is compensated by TRPC3 channel activity. Moreover, these findings imply that SERCA activity counteracts the ER Ca²⁺ leak in pancreatic β -cells by continuously sequestering entering Ca²⁺ into the ER lumen. To exclude that a reduced SERCA activity is itself responsible for the observed increased ER Ca²⁺ leak, ER Ca²⁺ refilling was determined directly after maximal ER Ca²⁺ depletion by a combination of histamine (in HeLa and EA.hy926 cells) or Cch (in INS-1 and MIN-6 cells) with the reversible SERCA inhibitor BHQ. In line with this, the ER Ca²⁺ refilling kinetics upon Ca²⁺ re-addition was comparable in all cell types tested (Fig. 4C, D). These findings exclude a reduced SERCA activity as the cause of the enhanced ER Ca²⁺ leakage in pancreatic β -cells.

The enhanced ER Ca²⁺ leakage in β -cells is mediated by presenilin-1

As it is known that presenilin-1 forms ER Ca²⁺ leak channels in several cell types [26, 27], we tested whether or not this protein is responsible for the enhanced ER Ca²⁺ leakage in β -cells. To this end, we examined the expression of presenilin-1 in the two pancreatic β -cell lines, INS-1 and MIN-6, as well as in HeLa and EA.hy926 using gene specific primers (Suppl. Table 1). Applying standard PCR the expression of presenilin-1 was verified in all cells used (Fig. 5A). Real-time PCR analysis revealed an equal gene expression of presenilin-1 in all four cell lines tested (Fig. 5B). To test whether or not presenilin-1 is functionally involved in the enhanced ER Ca²⁺ leakage in β -cells, we designed specific siRNAs to knockdown presenilin-1 in murine (MIN-6) and rat (INS-1) β -cells (Suppl. Table 1). Cell transfection with these siRNAs yielded an approximately 50 to 70 percent knockdown efficiency (Fig. 5C). Notably, siRNA-mediated knockdown of presenilin-1 abolished the enhanced ER Ca²⁺ leak in both β -cell lines (INS: Fig. 5D, F; Min-6: Fig. 5E, G) while no effect was observed in HeLa and EA.hy926 cells (Suppl. Fig. 3). To further verify the involvement of presenilin-1 in the enhanced ER Ca²⁺ leak in β -cells, we tested the effect of presenilin-1 overexpression. While an overexpression of presenilin-1 did not affect ER Ca²⁺ content in the presence of extracellular Ca²⁺ in none of the β -cells (Suppl Fig. 4A), overexpression of presenilin-1 resulted in a slight increase in the ER Ca²⁺ leakage in both β -cell lines (INS: Fig. 5D, F; Min-6: Fig. 5E, G) while the ER Ca²⁺ content in HeLa and EA.hy926 cells overexpressing presenilin-1 remained unaffected (Suppl. Fig. 4B).

Presenilin-1 dependent ER Ca²⁺ leak is independent of IP₃R expression

The involvement of inositol 1, 4,5-trisphosphate receptors (IP₃Rs) in presenilin-1-dependent ER Ca²⁺ leak is currently a matter of controversy [28–31]. Therefore, we tested for a possible involvement of IP₃Rs in the presenilin-1-dependent ER Ca²⁺ leak in INS-1. An initial expression analysis of all IP₃Rs indicated comparable expression of all three IP₃Rs in HeLa cells, while in the β-cell line, INS-1, the IP₃R type 3 was the by far most abundant IP₃R isoform (Suppl. Fig. 5). Based on these findings, we next attenuated the expression of IP₃R type 1 and 2, or that of IP₃R type 3 by specific siRNAs (Suppl. Fig. 6; for sequences see Suppl. Table 2). The efficiency of IP₃R knockdown was functionally confirmed by measuring Cch- or histamine-induced intracellular Ca²⁺ release using the Fura-2 technique (Suppl. Fig. 7). Neither a depletion of IP₃R type 1 and type 2 nor type 3 affected the ER Ca²⁺ leak in pancreatic β-cells, as shown by ER Ca²⁺ leak experiments (Fig. 5H). Likewise, knockdown of individual IP₃Rs also did not introduce an ER Ca²⁺ leak in HeLa cells (Suppl. Fig. 8). These findings suggest that none of the IP₃R subtypes is involved in the presenilin-1-dependent ER Ca²⁺ leak, which we found to be characteristic for β-cells and isolated islets.

GSK3β-mediated presenilin-1 phosphorylation drives the enhanced ER Ca²⁺ leakage in β-cells

Because expression levels of presenilin-1 in HeLa and EA.hy926 cells were comparable with that found in β-cells (Fig. 5B) and the overexpression of presenilin-1 did not introduce an enhanced ER Ca²⁺ leak in HeLa or EA.hy926 cells (Suppl. Fig. 4), we hypothesized that a post-translational modification of presenilin-1 was responsible for establishing the ER Ca²⁺ leakage in isolated pancreatic islets and β-cells. Notably, glycogen synthase kinase 3 beta (GSK3β)-mediated phosphorylation at serine 353 and serine 357 [32] of presenilin-1 is known to modulate its Ca²⁺ leak function [33]. Therefore, we explored the putative involvement of GSK3β in the enhanced ER Ca²⁺ leak found in the pancreatic islets and the two β-cell lines. Comparison of the expression level and activity of GSK3β in β-cells and the two non-β-cell lines revealed only slightly higher GSK3β expression in the two β-cell lines (Suppl. Fig. 9). However, an enzyme-linked immunosorbent assay [34] revealed strongly elevated GSK3β activity in both β-cell lines compared to the two other cell types (Fig. 6A). Accordingly, we hypothesized that an increased activity of GSK3β results in a hyperphosphorylation of presenilin-1 that, in turn, establishes increased ER Ca²⁺ leak.

To evaluate this hypothesis, isolated murine pancreatic islets and β-cells were pre-incubated for 24 or 48 h with the GSK3β inhibitor CHIR99021 [35] and the consequences thereof on the ER Ca²⁺ leak were investigated. Strikingly, inhibition of GSK3β prevented enhanced ER Ca²⁺ leak in the isolated pancreatic islets (Fig. 6B) and in both β-cell lines (Fig. 6C) but did not affect the ER Ca²⁺ content of the other cell types (Fig. 6D). Testing pancreatic islets viability revealed no toxic effect of CHIR99021 at the concentration and duration used (Suppl. Fig. 10). To further investigate the crucial role of GSK3β-mediated phosphorylation of presenilin-1 in the enhanced ER Ca²⁺ leak in β-cells we expressed a constitutively inactive presenilin-1 mutant with two alanines replacing the serine residues at position 353 and 357 (presenilin-1^{S353/357A}). Notably, presenilin-1^{S353/357A} cannot be phosphorylated by GSK3β. Expression of presenilin-1^{S353/357A} in the β-cells abolished the ER Ca²⁺ leak (Fig.

6E), thus, supporting our concept that GSK3 β -mediated serine phosphorylation of presenilin-1 accounts for the enhanced ER Ca²⁺ leak in this particular cell type.

To further substantiate the regulatory role of GSK3 β a constitutively active presenilin-1 mutant was used, in which the two serine residues at positions 353 and 357 were replaced by aspartic acids that mimic phosphorylated serines (presenilin-1^{S353/357D}). Expression of presenilin-1^{S353/357D} slightly enhanced the constitutive ER Ca²⁺ leak in INS-1 but not MIN-6 cells (Fig. 6F). However, in contrast to the findings in wild-type INS-1 and MIN-6 cells (Fig. 4C), the GSK3 β inhibitor CHIR99021 did not abolish the enhanced ER Ca²⁺ leak in β -cells expressing the phosphomimetic presenilin-1^{S353/357D} mutant (Fig. 6G). Notably, expression of constitutively active presenilin-1^{S353/357D} in HeLa and EA.hy926 cells introduced an enhanced ER Ca²⁺ leak, which was, in case of EA.hy926, comparable to that of wild-type β -cells (Fig. 6H). Together, these data demonstrate that GSK3 β -mediated phosphorylation of the two serine residues at positions 353 and 357 of presenilin-1 activates an ER Ca²⁺ leak and that hyperphosphorylated presenilin-1 establishes the augmented ER Ca²⁺ leak in pancreatic β -cells.

Mitochondria sequester Ca²⁺ leaked from the ER in β -cells

Our data above indicate that, despite a greatly enhanced ER Ca²⁺ leak in the pancreatic islets and β -cells, basal cytosolic Ca²⁺ does not differ from that found in the two other lines. However, basal ER Ca²⁺ levels were decreased in both β -cell lines compared to HeLa and EA.hy926 cells (Fig. 7A), despite SERCA activity is similar in all cell types (Fig. 4C,D). Considering the close proximity between the ER and mitochondria in nearly all cells including β -cells [36], it is tempting to speculate that mitochondria serve as “Ca²⁺ receiver” for the enhanced ER Ca²⁺ leak. In line with this hypothesis, resting mitochondrial Ca²⁺ levels were increased in the pancreatic β -cells compared to non- β -cells (Fig. 7B).

To investigate whether mitochondria indeed sequester most of the Ca²⁺ which leaks from the ER in pancreatic β -cells, mitochondrial Ca²⁺ uptake was prevented by siRNA-mediated knockdown of the mitochondrial Ca²⁺ uniporter (MCU) (Suppl. Fig. 11). In MCU depleted β -cells, the resting cytosolic Ca²⁺ levels were elevated compared to control cells (Fig. 7C). Moreover, resting mitochondrial Ca²⁺ levels and mitochondrial Ca²⁺ elevations upon stimulation with Cch and BHQ were reduced in MCU depleted β -cells (Suppl. Fig. 12). In contrast, reduction of MCU expression had no effect on basal cytosolic Ca²⁺ levels in non- β -cell lines (Fig. 7D). Notably, the inhibition of the β -cell-specific ER Ca²⁺ leakage by knockdown of presenilin-1, prevented the increase in basal cytosolic Ca²⁺ upon MCU knockdown in both β -cells (Fig. 7E). These data support our hypothesis that mitochondria effectively sequester the Ca²⁺ that leaks from the ER in pancreatic β -cells.

The tight dependency of resting mitochondrial Ca²⁺ from a continuous transfer of extracellular Ca²⁺, presumably via the enhanced ER Ca²⁺ leak was further illustrated by our findings that the removal of extracellular Ca²⁺ resulted in a small, biphasic yet significant decrease in mitochondrial Ca²⁺ levels in the INS-1 β -cell line (Fig. 7F, H) but not in non- β -cells (Fig. 7G, H).

The basal ER-to-mitochondria Ca^{2+} flux yields metabolic pre-activation of mitochondria in β -cells

To further reveal the functional consequences of an enhanced ER-to-mitochondria Ca^{2+} flux in β -cells, we measured mitochondrial respiration using the Seahorse[®] technology. Since, several dehydrogenases of the citric acid cycle are regulated by matrix Ca^{2+} elevation [37–39], we predicted that the constant Ca^{2+} uptake by mitochondria under resting conditions has a stimulatory effect on respiration. In line with this prediction, β -cells showed a considerably higher basal and maximal mitochondrial respiration compared to the non- β -cell lines (Fig. 8A). Manipulating the ER Ca^{2+} leakage by siRNA-mediated knockdown of presenilin-1 resulted in decreased basal and maximal respiration in the pancreatic β -cells (Fig. 8B), while the depletion of presenilin-1 had no effect on basal and maximal respiration in the other cell types (Suppl. Fig. 13).

In line with our experiments above that indicate that GSK3 β -induced phosphorylation of presenilin-1 accounts for the enhanced ER Ca^{2+} leak, the GSK3 β inhibitor CHIR99021 strongly decreased basal in both pancreatic β -cell lines (Fig. 8C, D). Similarly, CHIR99021 reduced maximal respiration in both pancreatic β -cell lines although only statistical significant in the INS-1 but not the MIN-6 cells (Fig. 8C, D). No effect on respiration was observed in the other cell types (Suppl. Fig. 14). These findings highlight that the functional coupling between enhanced ER Ca^{2+} leak and mitochondrial Ca^{2+} sequestration stimulates respiratory activity in the pancreatic β -cells.

To test whether or not the enhanced mitochondrial respiration that is due to the increased ER Ca^{2+} leak in β -cells is coupled to an enhanced basal ATP production in the mitochondria, basal mitochondrial ATP levels were measured using the genetically encoded and mitochondria-targeted ATP sensor, mtAT1.03 [40]. Compared to HeLa and EA.hy926 cells, both β -cell types showed elevated mitochondrial ATP levels under resting conditions (Fig. 8E). The siRNA-mediated reduction of the expression of presenilin-1 as well as the inhibition of GSK3 β with CHIR99021 reduced basal mitochondrial ATP levels in the pancreatic β -cells (Fig. 8F, G), whereas ATP levels within mitochondria of the non- β -cells cell types remained unaffected (Suppl. Fig. 15). Taken together, these data demonstrate that the enhanced ER Ca^{2+} leak and consequently increased mitochondrial Ca^{2+} sequestration yields an intrinsic pre-activation of mitochondrial respiration already under basal conditions.

Discussion

In the present study, we describe a cell type-specific, atypical ER Ca^{2+} leak in pancreatic β -cells under basal conditions. This continuous Ca^{2+} efflux from the ER in insulin secreting cells is established by GSK3 β -mediated phosphorylation of presenilin-1, is independent from IP₃-receptors, and is compensated by TRPC3-associated Ca^{2+} entry. Moreover, the Ca^{2+} leaking the ER is directly channeled towards the mitochondria in pancreatic β -cells and, subsequently, enhances basal Ca^{2+} , respiration and ATP levels in mitochondria. Accordingly, these data illustrate a tight functional coupling of ER Ca^{2+} leak with mitochondrial basal activity that appears specific for pancreatic β -cells.

Comparing isolated murine pancreatic islets and the two β -cell lines INS-1 and MIN-6 with two distinct, non- β cells (HeLa and EA.hy926) in this study, revealed strong ER Ca^{2+} leak only in the pancreatic islets and β -cells. The present study revealed that the ER Ca^{2+} loss in freshly isolated pancreatic islets and the two β -cell lines tested is compensated by ER refilling fueled by extracellular Ca^{2+} . The pharmacological profiling, together with our findings that a diminution of TRPC3 expression yields ER Ca^{2+} loss even in the presence of extracellular Ca^{2+} point to an involvement of TRPC3 in the continuous ER refilling process in the β -cells.

Our data show that the kinetics of Ca^{2+} refilling of emptied ER in the two β -cell lines and freshly isolated pancreatic islets are comparable to that found in the two cell lines that did not show enhanced ER Ca^{2+} leak (i.e. HeLa and EA.hy926). Therefore, a reduced SERCA activity as cause for the enhanced ER Ca^{2+} leakage in pancreatic islets/ β -cells can be excluded. There are several proteins known to establish an ER Ca^{2+} leak including Bcl-2 [41], pannexin 1 [42], TRPC1 [43], Sec61 [44] and presenilins [26, 27, 45]. Presenilins are enriched in mitochondrial-associated membranes (MAMs) [46] and have also been shown to foster ER-mitochondria coupling in a mitofusin-2-dependent manner [47]. There is an existing controversy concerning whether the presenilin-1-dependent ER Ca^{2+} leak occurs directly [26, 27] through presenilin-1 or whether the protein triggers flash-openings of IP_3Rs , especially of type 1 IP_3R [28–30]. Our data presented herein indicate that in β -cells the effect of presenilin-1 on ER Ca^{2+} leak is independent from the presence of any IP_3R . These findings favor either a direct function of presenilin-1 in β -cell ER Ca^{2+} leak or interactions with other ER Ca^{2+} channels. The lack of signs for involvement of IP_3Rs in the enhanced ER Ca^{2+} leak in β -cells might be due to the fact that all respective studies indicate type 1 IP_3R to be involved in presenilin-1-induced ER Ca^{2+} leak [30, 48, 49] while in pancreatic β -cells this particular type of IP_3R has lower expression compared to the predominantly expressed IP_3R type 3.

While our data strongly point to presenilin-1 being responsible for the ER Ca^{2+} leak found in pancreatic islets/ β -cells in line with our hypothesis, our data revealed and enhanced activity of GSK3 β , which is known to stimulate presenilin-1 Ca^{2+} leak [32], in the β -cells compared to non- β -cells. Although further studies are necessary, the various GSK3 β activities might be due to the differences in the energetic setting between the β -cells (INS-1, MIN-6), as being highly dependent on oxidative metabolism as basis of the sensory system for insulin secretion [3], and the highly glycolytic immortalized cell lines (HeLa, EA.hy926), which effectively operate under the Warburg effect [50]. Our data showing that GSK3 β inhibition abolished the ER Ca^{2+} leak in both β -cell lines and in isolated murine pancreatic islets, point to the involvement of GSK3 β -in the presenilin-1-mediated ER Ca^{2+} leak in β -cells. This assumption is further demonstrated by the utilization of constitutively active/inactive presenilin-1 mutants of serines at position 353 and 357 [32]. Similar findings were shown in cardiac myocytes where GSK3 β activity was found to establish an enhanced SR/ER-mitochondria Ca^{2+} crosstalk during reperfusion injury [49].

Our data further demonstrate that the leaked Ca^{2+} is rapidly sequestered by neighboring mitochondria and does not affect global cytosolic Ca^{2+} levels. This assumption builds on the increased resting Ca^{2+} levels in the mitochondrial matrix in β -cells and that the inhibition of

mitochondrial Ca^{2+} uptake by knockdown of MCU yielded increase in resting cytosolic Ca^{2+} levels only in the β -cells. Hence, inhibition of β -cell ER Ca^{2+} leak by either presenilin-1 knockdown or inhibition of GSK3 β by CHIR99021 prevented changes in cytosolic Ca^{2+} levels upon MCU depletion in both β -cell lines. Matrix Ca^{2+} is a major determinant for mitochondrial activity [6]. Notably, mitochondrial Ca^{2+} increase is known to stimulate matrix dehydrogenases of the citric acid cycle [37–39], thus, serving as a key trigger for insulin release in β -cells [51]. Our data that the ER Ca^{2+} leak yields increase in basal respiratory activity and mitochondrial ATP levels in β -cells are in line with this concept. Moreover, our data point to a continuous priming of β -cells based on a weak mitochondrial stimulation by the continuous Ca^{2+} flux from the ER as prerequisite for accurate responsiveness to elevated blood glucose sensing [13]. This conclusion is supported by our findings that inhibition of ER Ca^{2+} leak, either by diminution of presenilin-1 expression or inhibition of GSK3 β , abolished the enhanced respiratory activity and elevated mitochondrial ATP levels exclusively in the β -cells.

Familial Alzheimer's disease (AD) -linked presenilin-1 mutations have been described to disturb the Ca^{2+} leak function of the protein [27,31,52]. Notably, in several Alzheimer models, mutations in presenilins have been shown to yield Ca^{2+} accumulation in the ER [53], thus, pointing to a lack of ER Ca^{2+} leak function by the mutated presenilin-1. Accordingly, one may speculate that some cases of type 2 DM and familial AD might share the same molecular background: i.e. the lack of presenilin-1 established ER Ca^{2+} leak due to mutations either on the motifs responsible for the Ca^{2+} leak or on the phosphorylation sites for its regulator GSK3 β . In fact, the majority of familial AD patients also suffer from type 2 DM leading to the current understanding of type 2 DM as risk factor of AD [54]. Multiple studies raised epidemiological and experimental evidence for such possible shared pathophysiology between type 2 DM and AD [55] and link both diseases with mitochondrial dysfunction [56, 57]. So far many mechanisms have been discussed as common molecular causes of AD and type 2 DM [58]. Our present data indicate that certain mutations of presenilin-1, which alter the ER Ca^{2+} leak in neurons and pancreatic β -cells, impair respective cell functions and, hence, might cause the frequent coincidence of these severe diseases. Several reports describe disrupted interorganellar communication between the ER and mitochondria (MAMs) in AD [59–61]. Accordingly, though further studies are necessary, our present data and other reports point to deranged subcellular Ca^{2+} homeostasis due to mutations of presenilin-1 as a common molecular mechanism for reduced β -cells responsiveness leading to type 2 DM [62], as well as dysfunctional amyloid degradation causing AD [63].

Conclusion

Our data presented herein describe a GSK3 β /presenilin-1-dependent continuous ER Ca^{2+} leak in β -cells that yields priming of mitochondria by elevating organellar Ca^{2+} , increased basal respiration and ATP production. The physiological importance of such inter-organellar Ca^{2+} transfer and mitochondrial pre-activation awaits further investigations but might be related to β -cell responsiveness and/or insulin secretion.

Supplementary Material

Refer to Web version on PubMed Central for supplementary material.

Acknowledgements

We thank Mrs. Anna Schreilechner, BSc for expert assistance in cell culture.

Funding: This work was supported by the Austrian Science Funds (FWF; DKplus W 1226-B18 to W.F.G., P28529-B27 and I3716-B27 to R.M.; P28854 to T.M.), the Austrian Research Promotion Agency (FFG; 864690 to T.M.), the Austrian infrastructure program (HSRM 2016/201), the President's International Fellowship Initiative of CAS (No. 2015VBB045 to T.M.), and the National Natural Science Foundation of China (No. 31450110423 to T.M.). Microscopic equipment is part of the Nikon-*Center of Excellence*, Graz, supported by the HSRM 2013/2014, Nikon Austria, and BioTechMed. C.K. and B.G. are fellows of the Doctoral College "Metabolic and Cardiovascular Disease" at the Medical University of Graz funded by the FWF (W 1226-B18). W.F.G. is the guarantor of this work and, as such, had full access to all data in the study and takes responsibility for integrity of data and accuracy of data analyses. Author Contributions: C.K., B.G., M.W.-W. and M.R.D. performed calcium and ATP measurements, PCRs and ELISAs. C.T.M.S. performed respiration measurements. S.S. and T.M. performed and interpreted NMR data, V.S., M.D.-M. and D.K. isolated murine pancreatic islets, and, R.R. was responsible for cell culture. W.F.G. planned and supervised this work, and together with R.M. and J.H. prepared the manuscript. All authors discussed the results and implications and commented on the manuscript at all stages. Data availability: Supporting data are provided in the Supplementary Materials. Original data are available from the corresponding author upon request.

References

1. Trevisan R, Vedovato M, Tiengo A. The epidemiology of diabetes mellitus. *Nephrology Dialysis Transplantation*. 1998; 13:2–5.
2. Zheng Y, Ley SH, Hu FB. Global aetiology and epidemiology of type 2 diabetes mellitus and its complications. *Nat Rev Endocrinol*. 2018; 14:88–98. [PubMed: 29219149]
3. Maechler P, Wollheim CB. Mitochondrial signals in glucose-stimulated insulin secretion in the beta cell. *J Physiol (Lond)*. 2000; 529:49–56. [PubMed: 11080250]
4. Fu Z, Gilbert ER, Liu D. Regulation of insulin synthesis and secretion and pancreatic Beta-cell dysfunction in diabetes. *Curr Diabetes Rev*. 2013; 9:25–53. [PubMed: 22974359]
5. Wiederkehr A, Wollheim CB. Impact of mitochondrial calcium on the coupling of metabolism to insulin secretion in the pancreatic beta-cell. *Cell Calcium*. 2008; 44:64–76. [PubMed: 18191448]
6. Wiederkehr A, Szanda G, Akhmedov D, Matakı C, Heizmann CW, Schoonjans K, Pozzan T, Spät A, Wollheim CB. Mitochondrial matrix calcium is an activating signal for hormone secretion. *Cell Metab*. 2011; 13:601–611. [PubMed: 21531342]
7. Balaban RS. The role of Ca²⁺ signaling in the coordination of mitochondrial ATP production with cardiac work. *Biochim Biophys Acta*. 2009; 1787:1334–1341. [PubMed: 19481532]
8. McCormack JG, Halestrap AP, Denton RM. Role of calcium ions in regulation of mammalian intramitochondrial metabolism. *Physiol Rev*. 1990; 70:391–425. [PubMed: 2157230]
9. Baughman JM, Perocchi F, Girgis HS, Plovanich M, Belcher-Timme CA, Sancak Y, Bao XR, Strittmatter L, Goldberger O, Bogorad RL, Koteliansky V, et al. Integrative genomics identifies MCU as an essential component of the mitochondrial calcium uniporter. *Nature*. 2011; 476:341–345. [PubMed: 21685886]
10. De Stefani D, Raffaello A, Teardo E, Szabò I, Rizzuto R. A forty-kilodalton protein of the inner membrane is the mitochondrial calcium uniporter. *Nature*. 2011; 476:336–340. [PubMed: 21685888]
11. Perocchi F, Gohil VM, Girgis HS, Bao XR, McCombs JE, Palmer AE, Mootha VK. MICU1 encodes a mitochondrial EF hand protein required for Ca²⁺ uptake. *Nature*. 2010; 467:291–296. [PubMed: 20693986]
12. Alam MR, Groschner LN, Parichatikanond W, Kuo L, Bondarenko AI, Rost R, et al. Mitochondrial Ca²⁺ Uptake 1 (MICU1) and Mitochondrial Ca²⁺ Uniporter (MCU) Contribute to Metabolism-Secretion Coupling in Clonal Pancreatic β -Cells. *Journal of Biological Chemistry*. 2012; 287:34445–34454. [PubMed: 22904319]

13. Komatsu M, Takei M, Ishii H, Sato Y. Glucose-stimulated insulin secretion: A newer perspective. 2013; 4:511–516.
14. Asfari M, Janjic D, Meda P, Li G, Halban PA, Wollheim CB. Establishment of 2-mercaptoethanol-dependent differentiated insulin-secreting cell lines. *Endocrinology*. 1992; 130:167–178. [PubMed: 1370150]
15. Ishihara H, Asano T, Tsukuda K, Katagiri H, Inukai K, Anai M, Kikuchi M, Yazaki Y, Miyazaki JI, Oka Y. Pancreatic Beta-Cell Line Min6 Exhibits Characteristics of Glucose-Metabolism and Glucose-Stimulated Insulin-Secretion Similar to Those of Normal Islets. *Diabetologia*. 1993; 36:1139–1145. [PubMed: 8270128]
16. Scherer WF, Syverton JT, Gey GO. Studies on the propagation *in vitro* of poliomyelitis viruses. IV. Viral multiplication in a stable strain of human malignant epithelial cells (strain HeLa) derived from an epidermoid carcinoma of the cervix. *J Exp Med*. 1953; 97:695–710. [PubMed: 13052828]
17. Edgell CJ, McDonald CC, Graham JB. Permanent cell line expressing human factor VIII-related antigen established by hybridization. *Proc Natl Acad Sci USA*. 1983; 80:3734–3737. [PubMed: 6407019]
18. Madreiter-Sokolowski CT, Klec C, Parichatikanond W, Stryeck S, Gottschalk B, Pulido S, Rost R, Eroglu E, Hofmann NA, Bondarenko AI, Madl T, et al. PRMT1-mediated methylation of MICU1 determines the UCP2/3 dependency of mitochondrial Ca²⁺ uptake in immortalized cells. *Nat Comms*. 2016; 7
19. Alkan HF, Walter KE, Luengo A, Madreiter-Sokolowski CT, Stryeck S, Lau AN, Al-Zoughbi W, Lewis CA, Thomas CJ, Hoefler G, Graier WF, et al. Cytosolic Aspartate Availability Determines Cell Survival When Glutamine Is Limiting. *Cell Metab*. 2018; 28:706–720. [PubMed: 30122555]
20. Vinod M, Patankar JV, Sachdev V, Frank S, Graier WF, Kratky D, Kostner GM. miR-206 is expressed in pancreatic islets and regulates glucokinase activity. *Am J Physiol Endocrinol Metab*. 2016; 311:E175–E185. [PubMed: 27221121]
21. Madreiter-Sokolowski CT, Gy rffy B, Klec C, Sokolowski AA, Rost R, Waldeck-Weiermair M, Malli R, Graier WF. UCP2 and PRMT1 are key prognostic markers for lung carcinoma patients. *Oncotarget*. 2017; 8:80278–80285. [PubMed: 29113301]
22. Vishnu N, Jadoon Khan M, Karsten F, Groschner LN, Waldeck-Weiermair M, Rost R, Hallström S, Imamura H, Graier WF, Malli R. ATP increases within the lumen of the endoplasmic reticulum upon intracellular Ca²⁺ release. *Mol Biol Cell*. 2014; 25:368–379. [PubMed: 24307679]
23. Palmer AE, Jin C, Reed JC, Tsien RY. Bcl-2-mediated alterations in endoplasmic reticulum Ca²⁺ analyzed with an improved genetically encoded fluorescent sensor. *Proc Natl Acad Sci USA*. 2004; 101:17404–17409. [PubMed: 15585581]
24. Masumiya H, Shijuku T, Tanaka H, Shigenobu K. Inhibition of myocardial L- and T-type Ca²⁺ currents by efonidipine: possible mechanism for its chronotropic effect. *Eur J Pharmacol*. 1998; 349:351–357. [PubMed: 9671117]
25. Schleifer H, Doleschal B, Lichtenegger M, Oppenrieder R, Derler I, Frischauf I, Glasnov TN, Kappe CO, Romanin C, Groschner K. Novel pyrazole compounds for pharmacological discrimination between receptor-operated and store-operated Ca²⁺ entry pathways. *Br J Pharmacol*. 2012; 167:1712–1722. [PubMed: 22862290]
26. Tu H, Nelson O, Bezprozvanny A, Wang Z, Lee SF, Hao YH, Serneels L, De Strooper B, Yu G, Bezprozvanny I. Presenilins Form ER Ca²⁺ Leak Channels, a Function Disrupted by Familial Alzheimer's Disease-Linked Mutations. *Cell*. 2006; 126:981–993. [PubMed: 16959576]
27. Nelson O, Tu H, Lei T, Bentahir M, de Strooper B, Bezprozvanny I. Familial Alzheimer disease-linked mutations specifically disrupt Ca²⁺ leak function of presenilin 1. *J Clin Invest*. 2007; 117:1230–1239. [PubMed: 17431506]
28. Kasri NN, Kocks SL, Verbert L, Hébert SS, Callewaert G, Parys JB, Missiaen L, De Smedt H. Up-regulation of inositol 1, 4,5-trisphosphate receptor type 1 is responsible for a decreased endoplasmic-reticulum Ca²⁺ content in presenilin double knock-out cells. *Cell Calcium*. 2006; 40:41–51. [PubMed: 16675011]
29. Shilling D, Mak D-OD, Kang DE, Foskett JK. Lack of evidence for presenilins as endoplasmic reticulum Ca²⁺ leak channels. *J Biol Chem*. 2012; 287:10933–10944. [PubMed: 22311977]

30. Shilling D, Müller M, Takano H, Mak D-OD, Abel T, Coulter DA, Foskett JK. Suppression of InsP3 receptor-mediated Ca^{2+} signaling alleviates mutant presenilin-linked familial Alzheimer's disease pathogenesis. *J Neurosci*. 2014; 34:6910–6923. [PubMed: 24828645]
31. Nelson O, Supnet C, Tolia A, Horre K, de Strooper B, Bezprozvanny I. Mutagenesis Mapping of the Presenilin 1 Calcium Leak Conductance Pore. *J Biol Chem*. 2011; 286:22339–22347. [PubMed: 21531718]
32. Kirschenbaum F, Hsu SC, Cordell B, McCarthy JV. Substitution of a glycogen synthase kinase-3 β phosphorylation site in presenilin 1 separates presenilin function from beta-catenin signaling. *J Biol Chem*. 2001; 276:7366–7375. [PubMed: 11104755]
33. Twomey C, McCarthy JV. Presenilin-1 is an unprimed glycogen synthase kinase-3 β substrate. *FEBS Lett*. 2006; 580:4015–4020. [PubMed: 16814287]
34. Sutherland C, Leighton IA, Cohen P. Inactivation of glycogen synthase kinase-3 β by phosphorylation: new kinase connections in insulin and growth-factor signalling. *Biochem J*. 1993; 296:15–19. [PubMed: 8250835]
35. Cline GW, Johnson K, Regittnig W, Perret P, Tozzo E, Xiao L, Damico C, Shulman GI. Effects of a novel glycogen synthase kinase-3 inhibitor on insulin-stimulated glucose metabolism in Zucker diabetic fatty (fa/fa) rats. *Diabetes*. 2002; 51:2903–2910. [PubMed: 12351425]
36. Thivolet C, Vial G, Cassel R, Rieusset J, Madec AM. Reduction of endoplasmic reticulum-mitochondria interactions in beta cells from patients with type 2 diabetes. *PLoS ONE*. 2017; 12:e0182027. [PubMed: 28742858]
37. Robb-Gaspers LD, Burnett P, Rutter GA, Denton RM, Rizzuto R, Thomas AP. Integrating cytosolic calcium signals into mitochondrial metabolic responses. *EMBO J*. 1998; 17:4987–5000. [PubMed: 9724635]
38. Denton RM. Regulation of mitochondrial dehydrogenases by calcium ions. *Biochim Biophys Acta*. 2009; 1787:1309–1316. [PubMed: 19413950]
39. Rutter GA, McCormack JG, Midgley PJ, Denton RM. The role of Ca^{2+} in the hormonal regulation of the activities of pyruvate dehydrogenase and oxoglutarate dehydrogenase complexes. *Ann N Y Acad Sci*. 1989; 573:206–217. [PubMed: 2699397]
40. Imamura H, Nhat KPH, Togawa H, Saito K, Iino R, Kato-Yamada Y, Nagai T, Noji H. Visualization of ATP levels inside single living cells with fluorescence resonance energy transfer-based genetically encoded indicators. *Proc Natl Acad Sci USA*. 2009; 106:15651–15656. [PubMed: 19720993]
41. Foyouzi-Youssefi R, Arnaudeau S, Borner C, Kelley WL, Tschopp J, Lew DP, Demaurex N, Krause KH. Bcl-2 decreases the free Ca^{2+} concentration within the endoplasmic reticulum. *Proc Natl Acad Sci USA*. 2000; 97:5723–5728. [PubMed: 10823933]
42. Vanden Abeele F, Bidaux G, Gordienko D, Beck B, Panchin YV, Baranova AV, Ivanov DV, Skryma R, Prevarskaya N. Functional implications of calcium permeability of the channel formed by pannexin 1. *J Cell Biol*. 2006; 174:535–546. [PubMed: 16908669]
43. Berbey C, Weiss N, Legrand C, Allard B. Transient receptor potential canonical type 1 (TRPC1) operates as a sarcoplasmic reticulum calcium leak channel in skeletal muscle. *J Biol Chem*. 2009; 284:36387–36394. [PubMed: 19875453]
44. Lang S, Erdmann F, Jung M, Wagner R, Cavalie A, Zimmermann R. Sec61 complexes form ubiquitous ER Ca^{2+} leak channels. *Channels*. 2011; 5:228–235. [PubMed: 21406962]
45. Maesako M, Uemura K, Kuzuya A, Sasaki K, Asada M, Watanabe K, Ando K, Kubota M, Akiyama H, Takahashi R, Kihara T, et al. Gain of function by phosphorylation in Presenilin 1-mediated regulation of insulin signaling. *J Neurochem*. 2012; 121:964–973. [PubMed: 22443192]
46. Area-Gomez E, de Groof AJC, Boldogh I, Bird TD, Gibson GE, Koehler CM, Yu WH, Duff KE, Yaffe MP, Pon LA, Schon EA. Presenilins are enriched in endoplasmic reticulum membranes associated with mitochondria. *Am J Pathol*. 2009; 175:1810–1816. [PubMed: 19834068]
47. Filadi R, Greotti E, Turacchio G, Luini A, Pozzan T, Pizzo P. Presenilin 2 Modulates Endoplasmic Reticulum-Mitochondria Coupling by Tuning the Antagonistic Effect of Mitofusin 2. *Cell Rep*. 2016; 15:2226–2238. [PubMed: 27239030]

48. Cheung KH, Shineman D, Müller M, Cárdenas C, Mei L, Yang J, Tomita J, Iwatsubo T, Lee VM, Foskett JK. Mechanism of Ca^{2+} disruption in Alzheimer's disease by presenilin regulation of InsP3 receptor channel gating. *Neuron*. 2008; 58:871–883. [PubMed: 18579078]
49. Gomez L, Thiebaut P-A, Paillard M, Ducreux S, Abrial M, Crola Da Silva C, Durand A, Alam MR, Van Coppenolle F, Sheu SS, Ovize M. The SR/ER-mitochondria calcium crosstalk is regulated by GSK3 β during reperfusion injury. *Cell Death Differ*. 2016; 23:313–322. [PubMed: 26206086]
50. Depaoli MR, Karsten F, Madreiter-Sokolowski CT, Klec C, Gottschalk B, Bischof H, Eroglu E, Waldeck-Weiermair M, Simmen T, Graier WF, Malli R. Real-Time Imaging of Mitochondrial ATP Dynamics Reveals the Metabolic Setting of Single Cells. *Cell Rep*. 2018; 25:501–512.e1-e3. [PubMed: 30304688]
51. Maechler P, Wollheim CB. Role of mitochondria in metabolism-secretion coupling of insulin release in the pancreatic beta-cell. *Biofactors*. 1998; 8:255–262. [PubMed: 9914827]
52. Nelson O, Supnet C, Liu H, Bezprozvanny I. Familial Alzheimer's disease mutations in presenilins: effects on endoplasmic reticulum calcium homeostasis and correlation with clinical phenotypes. *J Alzheimers Dis*. 2010; 21:781–793. [PubMed: 20634584]
53. Zhang H, Sun S, Herreman A, de Strooper B, Bezprozvanny I. Role of presenilins in neuronal calcium homeostasis. *J Neurosci*. 2010; 30:8566–8580. [PubMed: 20573903]
54. Janson J, Laedtke T, Parisi JE, O'Brien P, Petersen RC, Butler PC. Increased risk of type 2 diabetes in Alzheimer disease. *Diabetes*. 2004; 53:474–481. [PubMed: 14747300]
55. Akter K, Lanza EA, Martin SA, Myronyuk N, Rua M, Raffa RB. Diabetes mellitus and Alzheimer's disease: shared pathology and treatment? *Br J Clin Pharmacol*. 2011; 71:365–376. [PubMed: 21284695]
56. Jha SK, Jha NK, Kumar D, Ambasta RK, Kumar P. Linking mitochondrial dysfunction, metabolic syndrome and stress signaling in Neurodegeneration. *Biochim Biophys Acta*. 2017; 1863:1132–1146.
57. Pugazhenti S, Qin L, Reddy PH. Common neurodegenerative pathways in obesity, diabetes, and Alzheimer's disease. *Biochimica et Biophysica Acta Mol Basis Dis*. 2017; 1863:1037–1045.
58. Kandimalla R, Thirumala V, Reddy PH. Is Alzheimer's disease a Type 3 Diabetes? A critical appraisal. *Biochim Biophys Acta*. 2017; 1863:1078–1089.
59. Schon EA, Area-Gomez E. Is Alzheimer's disease a disorder of mitochondria-associated membranes? *J Alzheimers Dis*. 2010; 20:S281–S292. [PubMed: 20421691]
60. Area-Gomez E, Schon EA. On the Pathogenesis of Alzheimer's Disease: The MAM Hypothesis. *FASEB J*. 2017; 31:864–867. [PubMed: 28246299]
61. Area-Gomez E, Schon EA. Mitochondria-associated ER membranes and Alzheimer disease. *Curr Opin Genet Dev*. 2016; 38:90–96. [PubMed: 27235807]
62. Davies MJ, Rayman G, Grenfell A, Gray IP, Day JL, Hales CN. Loss of the first phase insulin response to intravenous glucose in subjects with persistent impaired glucose tolerance. *Diabet Med*. 1994; 11:432–436. [PubMed: 8088119]
63. Xia W, Ostaszewski BL, Kimberly WT, Rahmati T, Moore CL, Wolfe MS, Selkoe DJ. FAD mutations in presenilin-1 or amyloid precursor protein decrease the efficacy of a gamma-secretase inhibitor: evidence for direct involvement of PS1 in the gamma-secretase cleavage complex. *Neurobiol Dis*. 2000; 7:673–681. [PubMed: 11114265]

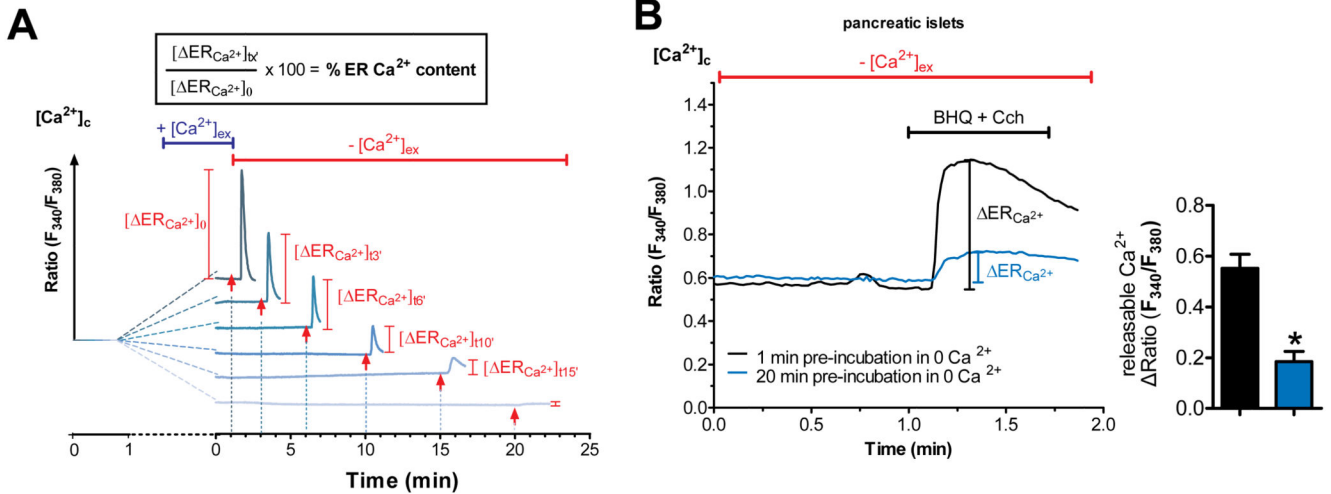


Fig. 1. Isolated pancreatic islets and β -cells have an atypical ER leak that is independent of SERCA activity.

(A) Schematic representation of the ER Ca^{2+} leakage protocol (original traces were from a respective experiment with INS cells). After loading cells with the cytosolic Ca^{2+} indicator Fura-2/AM, they were perfused with Ca^{2+} containing EB for 1 min before switching to Ca^{2+} -free buffer for predefined periods of time i.e. 1, 3, 6, 10, 15 and 20 min. For evaluation of ER Ca^{2+} content, ER Ca^{2+} stores were fully depleted by applying IP_3 -generating agonists (100 μ M carbachol for pancreatic islets/ β -cells or histamine for non- β -cells) together with 15 μ M of the SERCA inhibitor BHQ – to avoid refilling of the ER – at the time points indicated with an arrow. The maximal ER store depletion was measured as maximal releasable ER Ca^{2+} in the cytosol whereas the ER is considered as fully filled at the one min time point and used as reference for calculating ER Ca^{2+} content. (B) Representative curves showing ER Ca^{2+} content indirectly measured with Fura-2/AM in isolated pancreatic islets. Islets were kept in Ca^{2+} -free buffer for 1 min (black line) or 20 min (blue line) prior to ER Ca^{2+} store depletion by applying the SERCA inhibitor BHQ (15 μ M) together with carbachol (Cch, 100 μ M). Bars on the right represent corresponding statistics. * $p < 0.05$ tested with unpaired Student's t-test, n = 4.

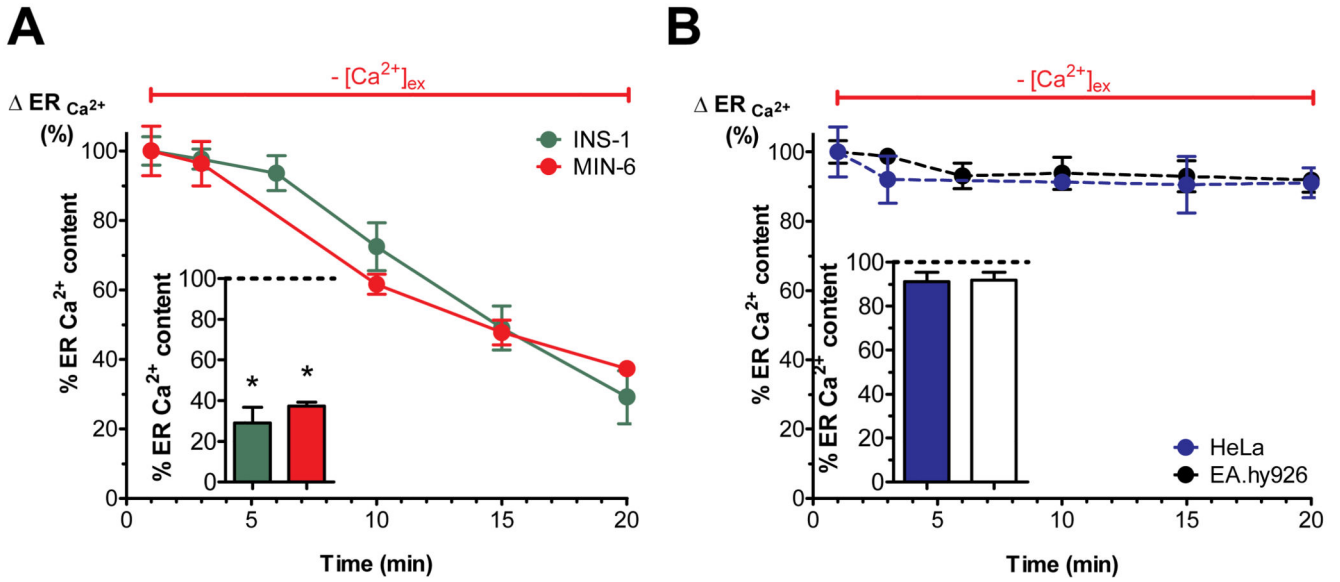


Fig. 2. Isolated pancreatic islets and β -cells have an atypical ER leak that is independent of SERCA activity.

(A,B) Percentage of ER Ca^{2+} leak, representing the maximal amount of Ca^{2+} released from the ER, under Ca^{2+} -free conditions stimulated with the IP_3 -generating agonists (A) carbachol (100 μM) in MIN-6 (red values) and INS-1 cells (green values) together with the SERCA-inhibitor BHQ (15 μM) or (B) histamine (100 μM) in HeLa (blue values) and EA.hy926 cells (black values) at the indicated time points. Bar charts represent the percentage of ER Ca^{2+} content after 20 min of incubation under Ca^{2+} -free conditions. The corresponding 1 min value was set to 100% (n = 6). * $p < 0.05$ using one-way ANOVA.

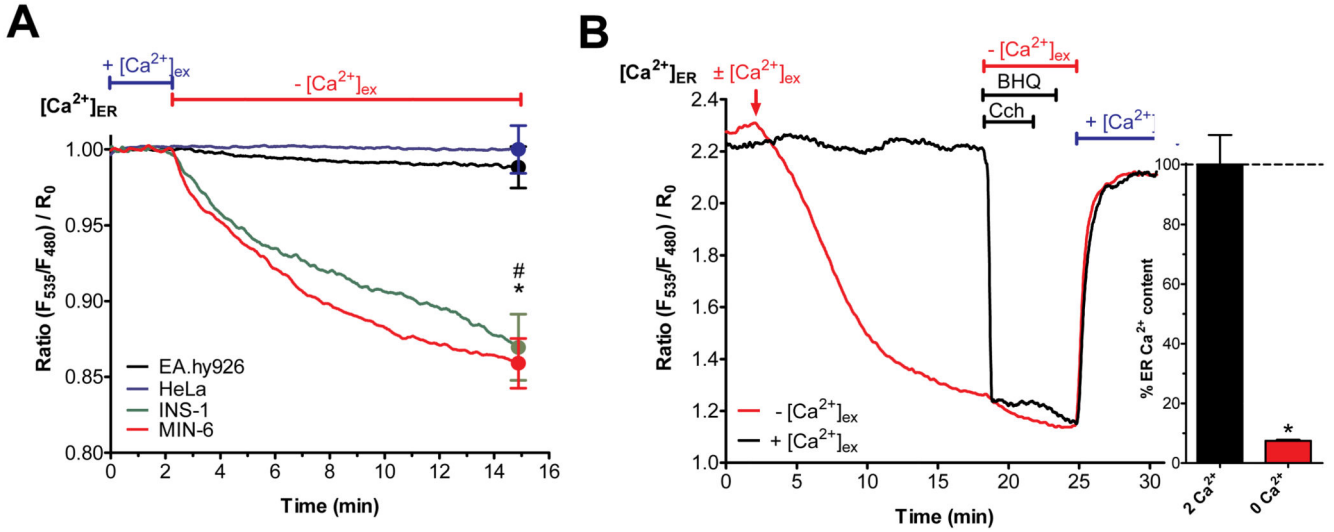


Fig. 3. Isolated pancreatic islets and β -cells have an atypical ER leak that is independent of SERCA activity.

(A) Curves reflect normalized $[Ca^{2+}]_{ER}$ ratio signals over time measured with the genetically encoded Ca^{2+} probe D1ER in HeLa (blue curve), EA.hy926 (black curve), INS-1 (green curve) and MIN-6 (red curve) cells perfused with experimental buffer containing 2 mM Ca^{2+} for two min before switching to 0 mM Ca^{2+} and EGTA-containing buffer (n = 6). (B) Representative curves for β -cells (depicted INS-1) reflect $[Ca^{2+}]_{ER}$ ratio signals over time in the presence (2 mM Ca^{2+} ; black curve) or absence (0 mM Ca^{2+} ; red curve) of Ca^{2+} measured with D1ER. The ER Ca^{2+} store was depleted using carbachol (100 μ M) and BHQ (15 μ M) in Ca^{2+} -free EGTA-buffered solution prior to addition of 2 mM external Ca^{2+} (n = 6).

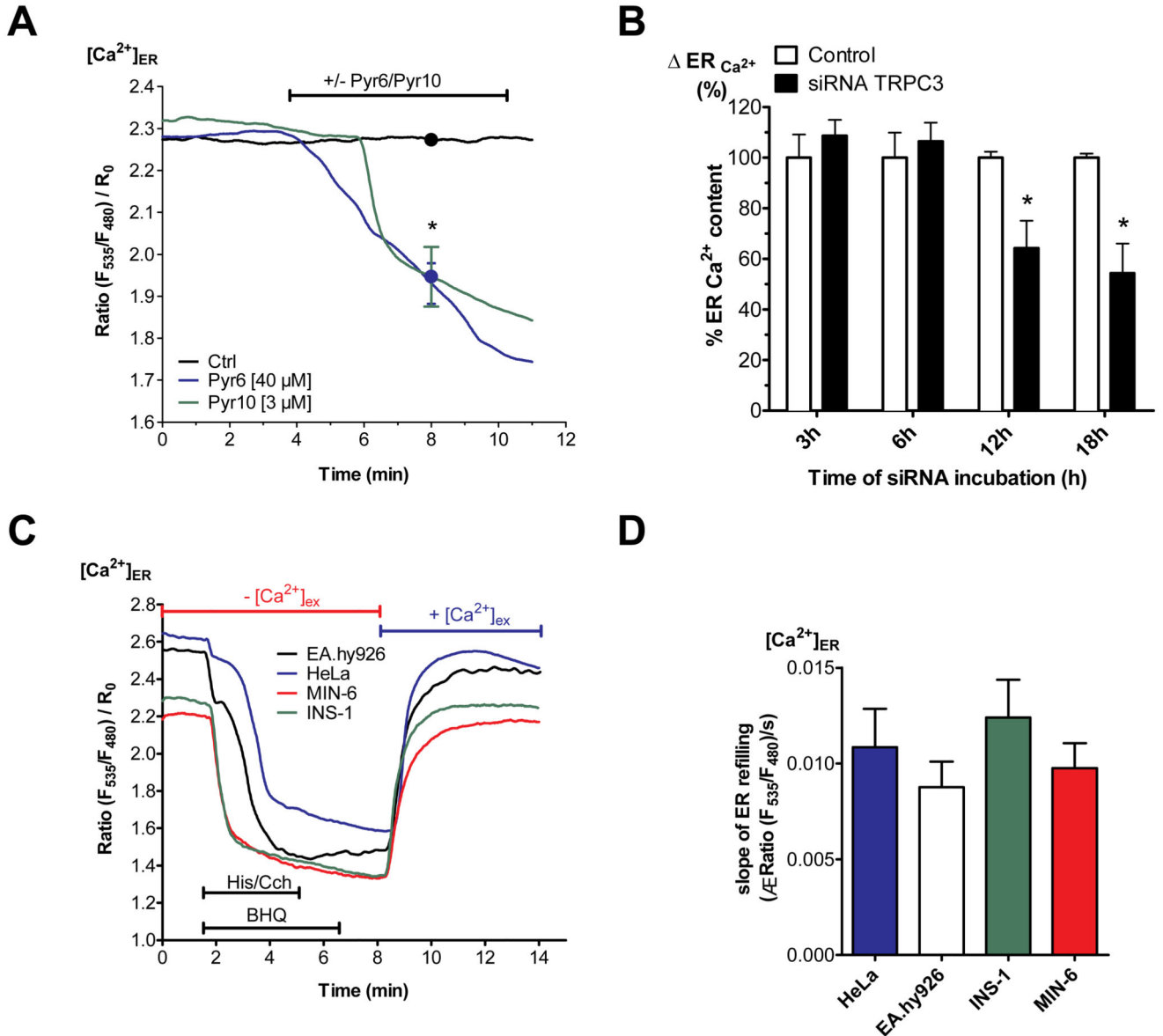


Fig. 4. Enhanced ER Ca^{2+} loss in β -cells is compensated by TRPC3-associated Ca^{2+} entry. (A) Curves for β -cells (depicted INS-1) reflect $[Ca^{2+}]_{ER}$ ratio signals over time measured with D1ER in experimental buffer containing 2 mM Ca^{2+} under control conditions (black curve), with the TRPC3 inhibitor Pyr6 (40 μ M) or Pyr10 (3 μ M) (n = 6). (B) Percentage of ER Ca^{2+} content under Ca^{2+} -free conditions in INS-1 cells under control conditions (white bars) or 3, 6, 12 or 18 h after transfection with specific siRNA against of TRPC3 (white bars). ER Ca^{2+} content was measured by applying the SERCA inhibitor BHQ (15 μ M), together with carbachol (100 μ M). The corresponding 1 min control values were set to 100%. * $p < 0.05$, tested with one-way ANOVA (n=6). (C) Representative traces and respective statistic (D) illustrating $[Ca^{2+}]_{ER}$ over time in HeLa (blue line), EA.hy926 (black line), INS-1 (green line) and MIN-6 (red line) cells, measured by D1ER (Data extracted from D). ER Ca^{2+} store was depleted using 100 μ M histamine (His) for

HeLa and EA.hy926 or 100 μM carbachol (Cch) for INS-1 and MIN-6 together with 15 μM BHQ in Ca^{2+} -free EGTA-buffered solution. To compare SERCA activity between the cell lines, external Ca^{2+} (2 mM) was added after agonists were washed out. Bars on the right represent corresponding statistics (n = 6).

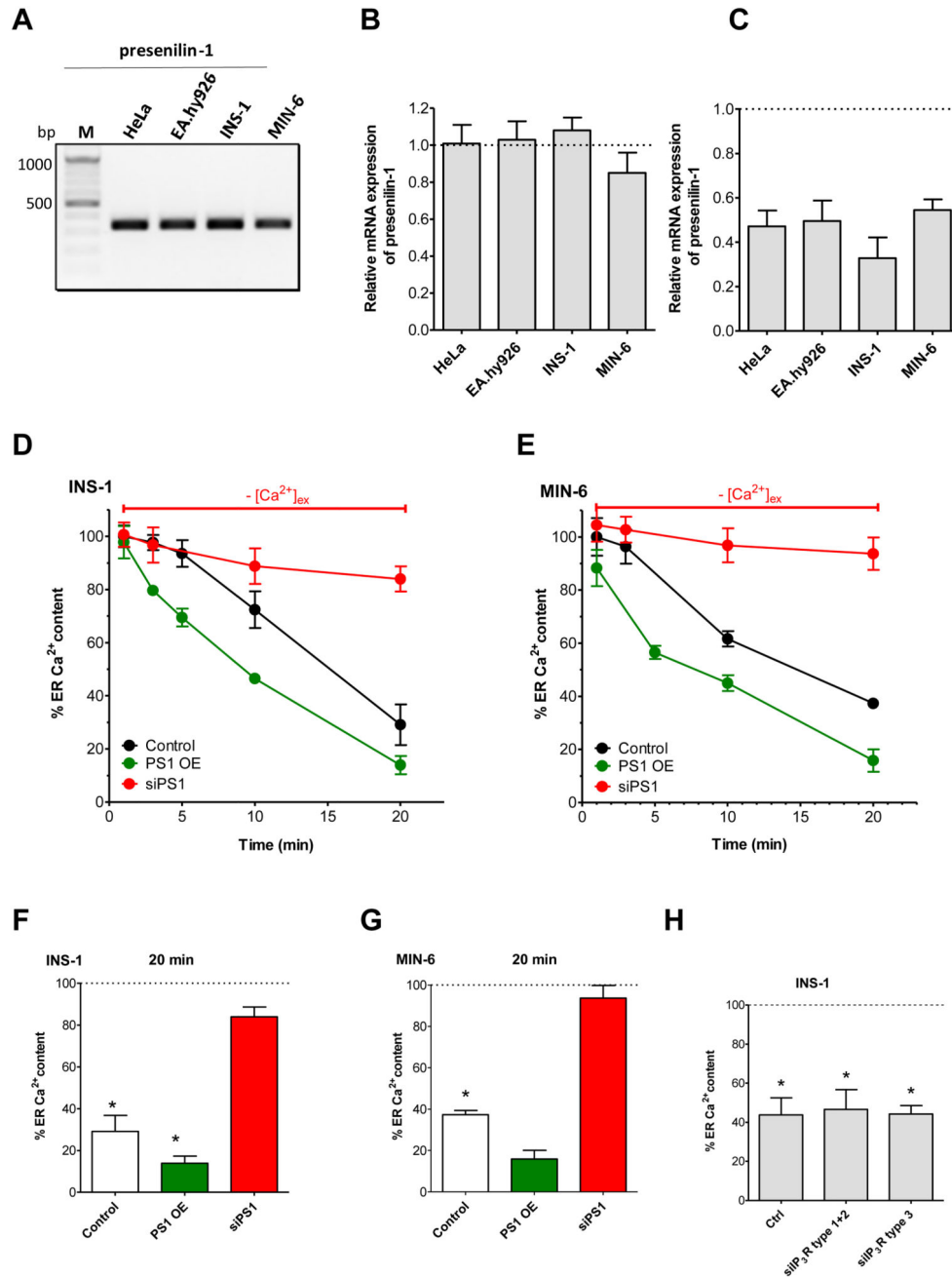


Fig. 5. Enhanced ER Ca²⁺ loss in β -cells is due to presenilin-1.

(A) Representative gel showing detection of mRNA levels of presenilin-1 in HeLa, EA.hy926, INS-1 and MIN-6 cells via standard PCR using gene and species specific primers (n = 3). (B) Quantification of mRNA expression levels of presenilin-1 in HeLa, EA.hy926, INS-1 and MIN-6 cells compared to mRNA levels of the housekeeping gene GAPDH detected with qPCR (n = 3). Bar charts indicate mean + SEM. (C) Quantification of knockdown efficiency of presenilin-1 in HeLa, EA.hy926, INS-1 and MIN-6 cells compared to the housekeeping gene GAPDH using real-time PCR (n = 3). (D,E) Evaluation of the

influence of presenilin-1 knockdown (siPS1) and over-expression (PS1 OE) on ER Ca^{2+} leakage – depicted as percentage of the initial ER Ca^{2+} content in (D) INS-1 and (E) MIN-6 under control conditions (black lines), upon knockdown of presenilin-1 (red lines) or over-expression of presenilin-1 (green lines) after incubation under Ca^{2+} -free conditions. ER Ca^{2+} stores were depleted at the indicated time by treating the cells with 15 μM of the SERCA inhibitor BHQ and 100 μM carbachol. Points represent the mean values \pm SEM (n = 6). (F) Corresponding statistics for panels D and E showing the % of ER Ca^{2+} content in INS-cells (upper panel) and MIN-6 cells (lower panel) after 20 min incubation in Ca^{2+} -free buffer and after ER Ca^{2+} stores were depleted by 100 μM Cch and 15 μM BHQ. Respective 1 min values were set to 100%. Bars represent mean \pm SEM (n = 6). * $p < 0.05$ versus respective 1 min control or as indicated in the graph using one-way ANOVA. (G) Percentage of ER Ca^{2+} content in INS-1 cells after 20 min of incubation under Ca^{2+} -free conditions either under control conditions or after knockdown of the indicated types of IP_3R . ER stores were depleted after 20 min by applying 0.2 μM of ionomycin together with the SERCA inhibitor BHQ (15 μM). In each graph the 1 min control value was set to 100% (n = 5). * $p < 0.05$ versus respective 1 min control or as indicated in the graph using one-way ANOVA. (H) Percentage of ER Ca^{2+} content in INS-1 cells after 20 min of incubation under Ca^{2+} -free conditions either under control conditions or after knockdown of the indicated types of IP_3R . ER stores were depleted after 20 min by applying 0.2 μM of ionomycin together with the SERCA inhibitor BHQ (15 μM). In each graph the 1 min control value was set to 100% (n = 5). * $p < 0.05$ versus respective 1 min control or as indicated in the graph using one-way ANOVA.

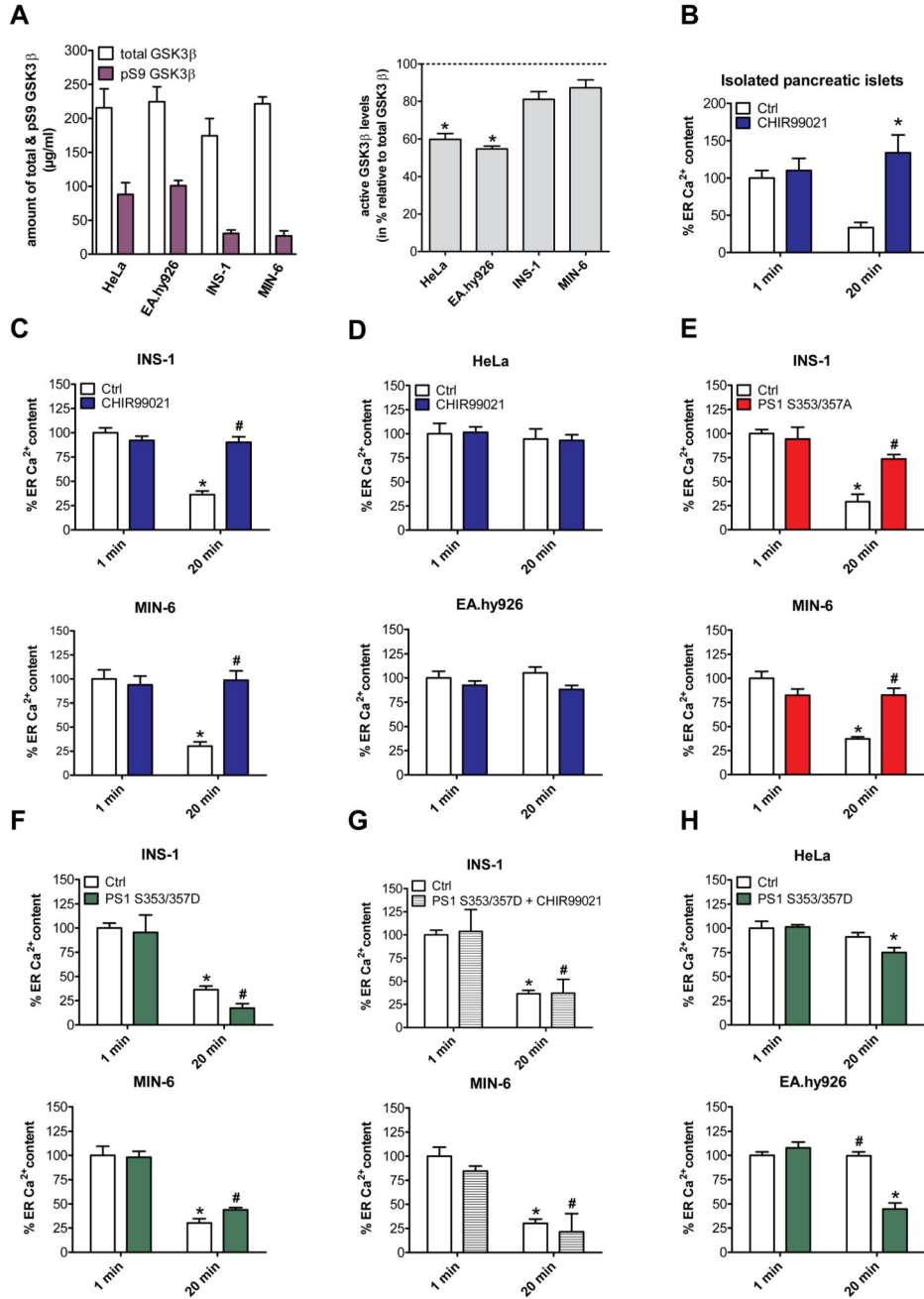


Fig. 6. GSK3β regulates presentin-1-dependent ER Ca²⁺ leakage in pancreatic islets and β-cells. (A) Left panel: Quantification of the levels of total GSK3β and its inactive version pS9 GSK3β in MIN-6, INS-1, EA.hy926 and HeLa cells. Right panel: Ratio of active GSK3β versus total GSK3β in MIN-6, INS-1, EA.hy926 and HeLa cells using a specific ELISA (n 4). *p<0.05 refers to active levels of EA.hy926 and HeLa compared to β-cells. (B-H) Percentage of ER Ca²⁺ content in EB and after 20 min in Ca²⁺-free EB. At the indicated time points ER Ca²⁺ stores were depleted using the SERCA inhibitor BHQ (15 μM), together with histamine (100 μM) for HeLa and EA.hy926 cells or carbachol (100 μM) for

INS-1, MIN-6 cells and isolated murine pancreatic islets. (B) Percentage of ER Ca²⁺ content in isolated murine pancreatic islets under control conditions (white bars) or after treatment with the GSK3 β inhibitor CHIR99021 (2.5 μ M) for 24 h (blue bars). (C) Percentage of ER Ca²⁺ content in INS-1 (upper panel) and MIN-6 cells (lower panel) as well as (D) in HeLa (upper panel) and EA.hy926 cells (lower panel) under control conditions (white bars) and after treatment with the GSK3 β inhibitor CHIR99021 (2.5 μ M) for 48 h (blue bars). (E) Percentage of ER Ca²⁺ content in INS-1 (upper panel) and MIN-6 cells (lower panel) under control conditions (white bars) or after overexpression of presenilin-1 mutated version which cannot be phosphorylated (PS1 S353/357A) (red bars). (F) Percentage of ER Ca²⁺ content in INS-1 (upper panel) and MIN-6 cells (lower panel) under control conditions (white bars) or after overexpression of a constitutively active presenilin-1 mutated version (PS1 S353/357D) (green bars). (G) Percentage of ER Ca²⁺ content in INS-1 (upper panel) and MIN-6 cells (lower panel) under control conditions (white bars) or after a combination of overexpression of PS1 S353/357D and treatment with 2.5 μ M of the GSK3 β inhibitor CHIR99021 (striped bars). (H) Percentage of ER Ca²⁺ content in HeLa (upper panel) and EA.hy926 cells (lower panel) under control conditions (white bars) or after overexpression of PS1 S353/357D (grey bars). Bars represent mean \pm SEM. In each graph the 1 min control value was set to 100% (n = 6). *p<0.05 versus respective 1 min control or as indicated in the graph using one-way ANOVA.

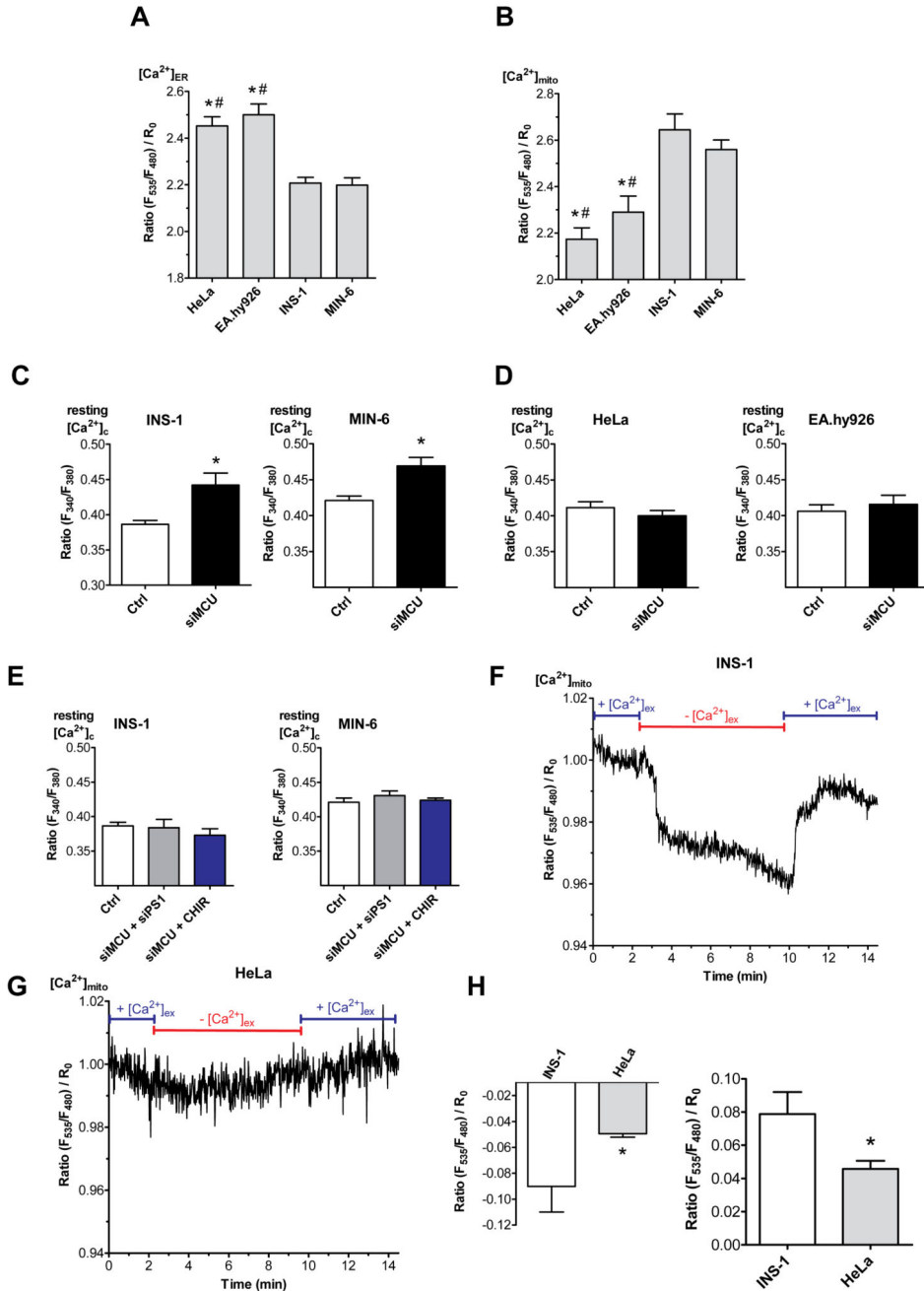


Fig. 7. Mitochondria serve as Ca^{2+} sink for ER leakage.

(A,B) Bars represent basal ratios of $[Ca^{2+}]_{ER}$ measured with D1ER (A) or $[Ca^{2+}]_{mito}$ measured with mito 4mtD3cpv (B) in HeLa, EA.hy926, INS-1 and MIN-6 cells. Bar charts indicate mean \pm SEM (n = 6). * $p < 0.05$ versus INS-1; # $p < 0.05$ versus MIN-6 using one-way ANOVA. (C-F) Bars represent the basal ratio of $[Ca^{2+}]_{cyto}$ measured with Fura-2/AM under Ca^{2+} -free conditions in (C,E) INS-1 and MIN-6 cells as well as (D,F) in HeLa and EA.hy926 cells under control conditions (white bars) and siRNA against MCU (black bars) (C,D), as well as under control conditions (white bars), a combination of siRNA against

MCU and PS1 (grey bars) and a combination of siRNA against MCU and treatment with CHIR99021 (2.5 μM ; blue bars) (E) (n = 6). * $p < 0.05$ versus control using the unpaired Student's t-test and also with one way ANOVA where applicable. (F,G) Normalized $[\text{Ca}^{2+}]_{\text{mito}}$ ratio signals measured over time in INS-1 (F) as well as in HeLa (G) in 2 mM Ca^{2+} (2Ca^{2+}) containing or Ca^{2+} -free-EGTA buffered solution as indicated in the graph. To visualize the max. mitochondrial Ca^{2+} uptake and proper functionality of the sensor cells were stimulated with 100 μM carbachol (Cch) for β -cells and 100 μM histamine (His) for non- β -cells together with 15 μM BHQ. (H) Statistics on the absolute drop in mitochondrial Ca^{2+} upon removal of extracellular Ca^{2+} (left panel) and the rise in mitochondrial Ca^{2+} after re-addition of extracellular Ca^{2+} (right panel). * $p < 0.05$ versus β -cells using the unpaired Student's t-test (n = 6).

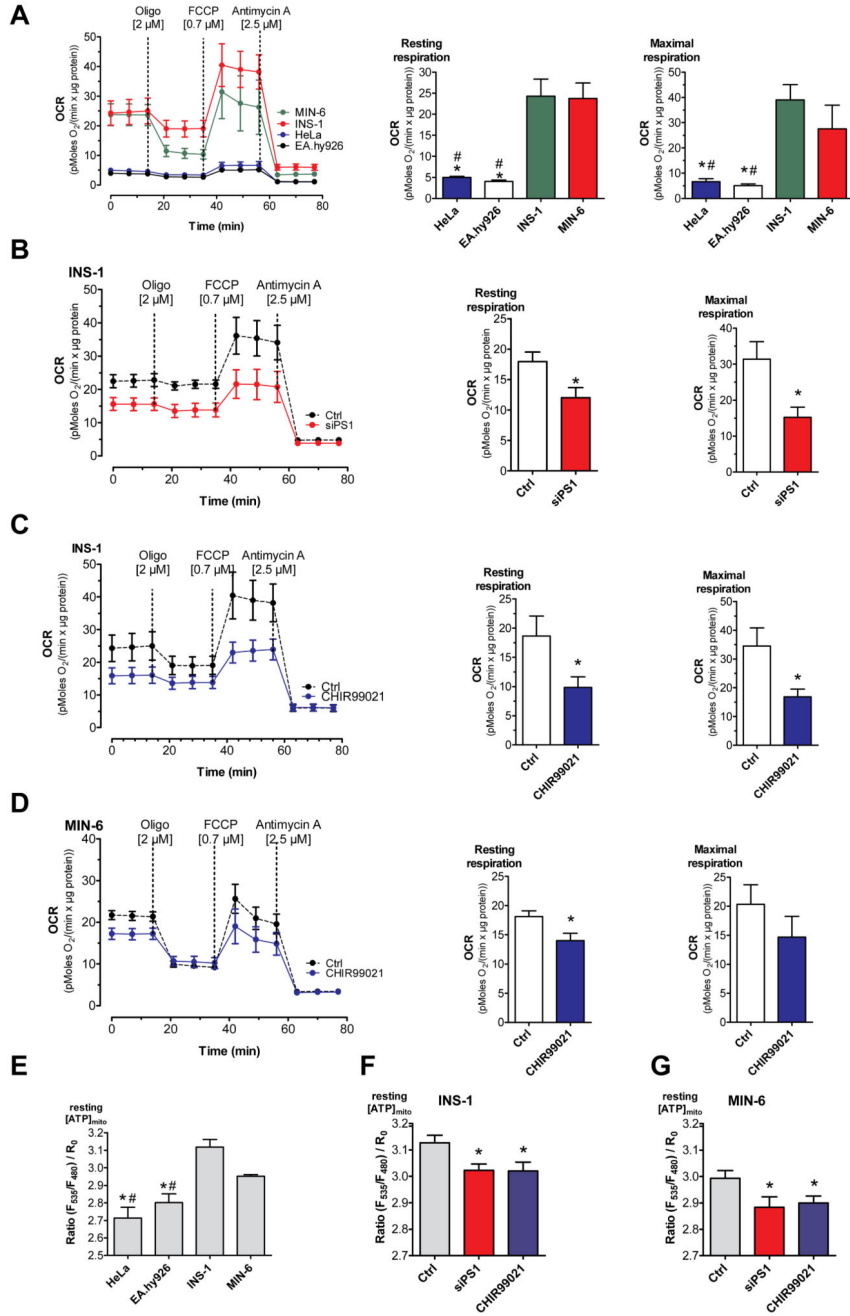


Fig. 8. ER Ca²⁺ leak fuels increased basal mitochondrial activity.

(A) The mitochondrial respiration (OCR) in β -cells (INS-1: green line; MIN-6: red line) compared with that of non- β -cells (HeLa: blue line; EA.hy926: black line) under resting conditions. Bars on the right represent corresponding statistics of the resting (middle panel) and maximal OCR (right panel), mean \pm SEM, * $p < 0.05$ compared to INS-1, # $p < 0.05$ compared to MIN-6 tested with one-way ANOVA. (B) OCR of INS-1 cells under control conditions (black dotted line) and knockdown of presenilin-1 (red line), bars represent corresponding basal and maximal respiration. (C,D) OCR of INS-1 cells (C) and MIN-6

cells (D) under control conditions (black line) or after treatment with the specific GSK3 β inhibitor CHIR99021 for 48 h (blue line). Bars on the right represent basal and maximal respiration under control conditions (white bars) and after treatment with CHIR99021 (blue bars). (A-D) OCR was normalized to protein content. As indicated, cells were treated with 2 μ M oligomycin, 0.7 μ M FCCP for INS-1, EA.hy926 and MIN-6 and 0.3 μ M for HeLa, and 2.5 μ M antimycin A. Data present the mean values \pm SEM (n=6). *p<0.05 versus control using the unpaired Student's t-test. (E-G) Bars represent basal [ATP]_{mito} ratio measured with mtAT1.03 in HeLa, EA.hy926, INS-1 and MIN-6 cells under control conditions (E), or after knockdown of presenilin-1 (red bars) and prior treatment with 2.5 μ M of the GSK3 β inhibitor CHIR99021 (blue bars) in INS-1 (F) or MIN-6 (G) cells (n = 6). #p<0.05 HeLa and EA.hy926 vs MIN-6 or *p<0.05 HeLa and EA.hy926 vs INS-1 in 5E or versus control in 5F and 5G using the unpaired Student's t-test or one way ANOVA where applicable (n=6).